CdL Scienza dei Materiali - Fisica delle Nanotecnologie - a.a. 2003/4

Appunti & trasparenze - Parte 7

Versione 2, Novembre 2003
Francesco Fuso, tel 0502214305, 0502214293 - fuso@df.unipi.it
http://www.df.unipi.it/~fuso/dida

Problematiche di crescita di film sottili; alcuni metodi fisici e chimici di deposizione e crescita di film sottili: MBE, MOMBE, Sputtering, PLAD, CVD, LPE, ...

11/11/2003 - 9.30+1 ITI G (Andrea CAMPOSEO)

Crescita epitassiale

Generalmente l'obiettivo è un film sottile (typ. spessore max ~µm) cristallino (es. semiconduttori, alcuni metalli,...) o policristallino (es. alcuni ossidi, ceramiche,…)

Crescita (etero)epitassiale: ordine piani reticolari lungo l'asse *c* (per cristalli, ordine anche nel piano *ab*, cioè tessitura biassiale)

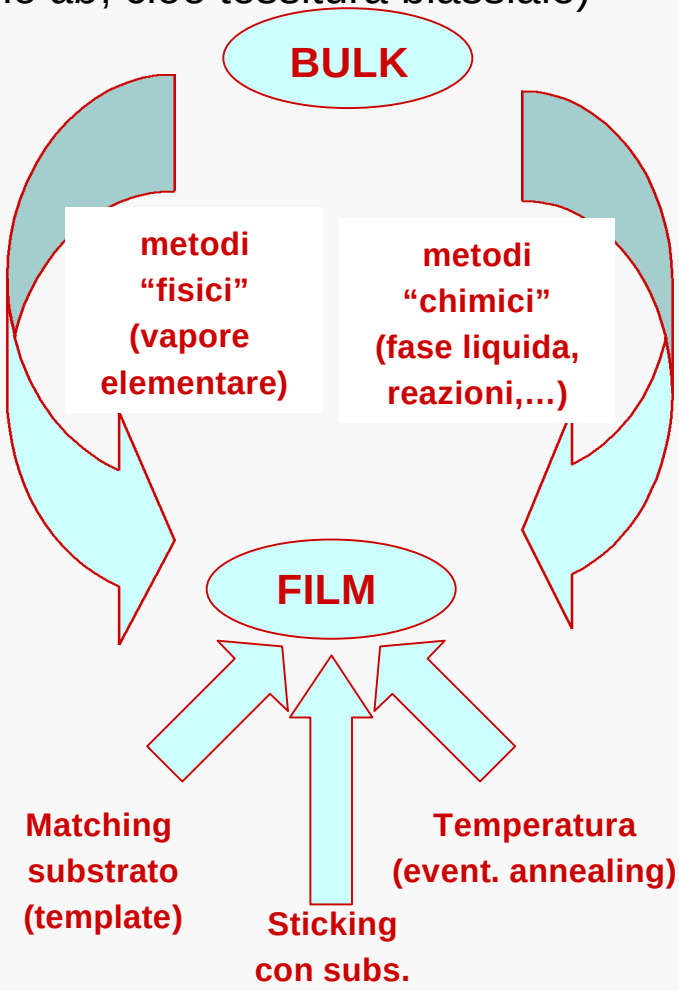

Lattice matching

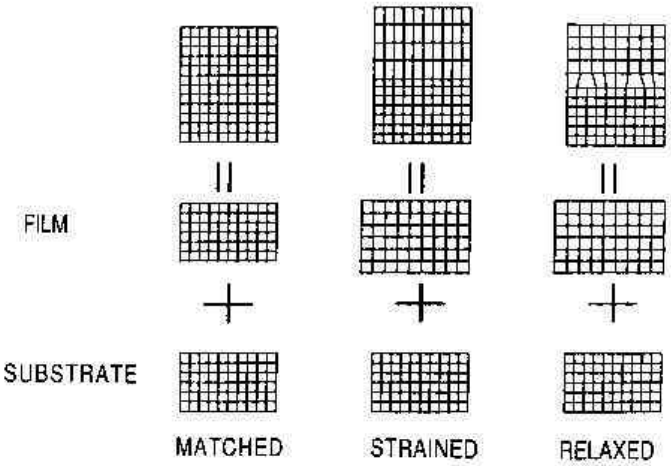

Figure 7-1. Schematic illustration of lattice-matched, strained, and relaxed hetei taxial structures. Homoepitaxy is structurally very similar to lattice-matched hetei taxy.

Growth and defects

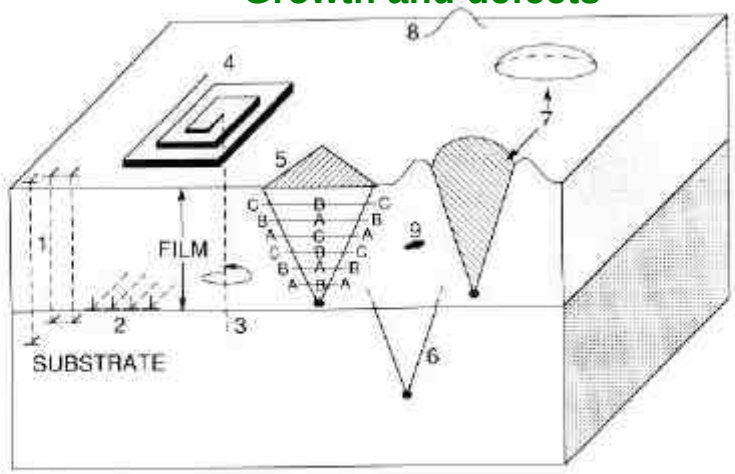

Figure 7-10. Schematic composition of crystal defects in eptiaxial films: (1) thread- ing edge dislocations; (2) interfacial misfit dislocations; (3) threading screw dislocation; (4) growth spiral; (5) stacking fault in film; (6) stacking fault in substrate; (7) oval defect; (8) hillock; (9) precipitate or void.

Interazione particelle/substrato I: diffusione

La diffusione delle particelle che arrivano sul substrato (elemento essenziale per avere copertura omogenea e formazione del film) è controllata da temperatura e da barriere di energia per muoversi su una “piattaforma”, salire o scendere tra “piattaforme” diverse

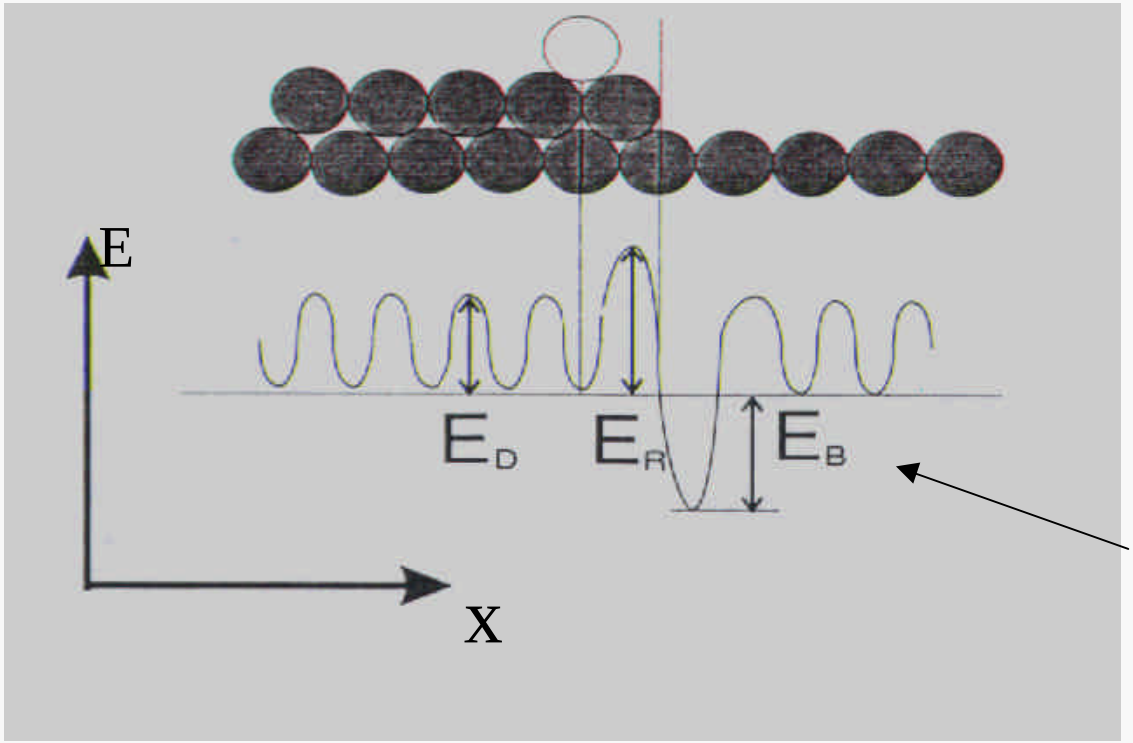

Coefficiente di diffusione:

$D = D_0 \exp(-E/kT)$

Barriera di Schwoebel:
energie diverse localmente

Interazione particelle/substrato II: nucleazione

Nucleation

This phase of growth is based on spontaneous formation of aggregate of atoms which is large enough to be energetically stable.
This condition is reached when the gain in volume energy for an additional monomer exceeds the energy loss due to surface formation

Kinetic concept (Venable's model)

Critical cluster of size i* : *adding a further monomer to a critical cluster leads to a stable cluster which does not decompose anymore.*

Assumptions

1. All stable clusters can be considered a group in the form $N_x = \sum_{j=1^*+1}^{\infty} N(j)$

2. The number of subcritical clusters reaches a steady-state

Rate equations

$$\frac{dn}{dt} = F - \frac{n}{\tau} - \frac{d}{dt} j_x N_x$$

$$\frac{dN(j)}{dt} = 0 \quad \text{For } 1<j<i^*$$

$$\frac{dN_x}{dt} = n\sigma_m(i^*)N(i^*) - 2N_x\frac{d\vartheta}{dt}$$

$$\vartheta = Aj_x N_x$$

Materiale tratto dal seminario di Barbara Fazio
IPCF/CNR Messina, Aprile 2003

Coalescence

During a film growth process, when the experimental conditions past the nucleation regime and favor merging of clusters, the system continues to evolve towards a coalescence morphology.

In this regime has been characterized the following three cluster growths (Beysens et al.):

- ***Nucleation and individual cluster growth without cluster density reduction or pre-coalescence and transient coalescence stage (diffusive mass transport limited growth)***
- ***Cluster merging or late stage of coalescence (static and dynamic)***
- ***Secondary nucleation and cluster growth on exposed fraction of surface.***

Esempio di studio di coalescenza (fasi iniziali della crescita)

Experimental study of coalescence regime in the system Ga on GaAs(001)

(M.Zinke-Allmang et al.)

- ***Base pressure $<5*10^{-9}$ Pa***
- ***Deposition equivalent to a coverage of about 13 monolayers at room temperature.***
- ***Annealing temperature = 660°C for 5 min.***

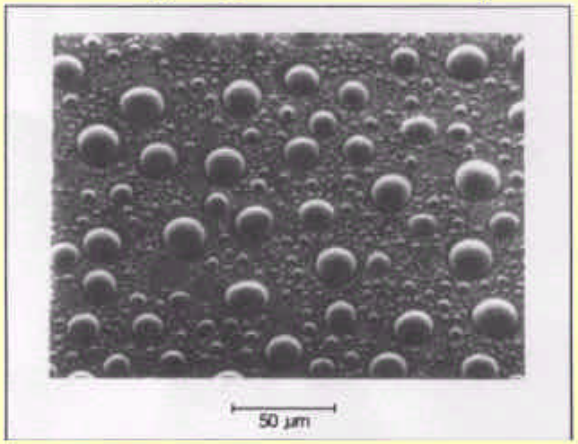

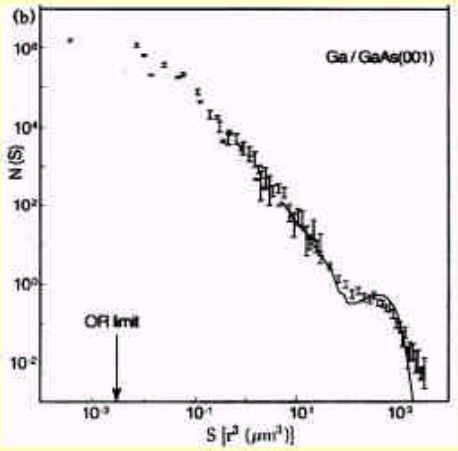

Good agreement between experimental results and theoretical model of coalescence regime (even if microscopic details in Monte Carlo simulations differ from the experiment quite substantially)

Coalescenza/nucleazione: processi concorrenti

Dipendenza da caratteristiche del substrato (diffusione)

Vaporizzazione (effusiva)

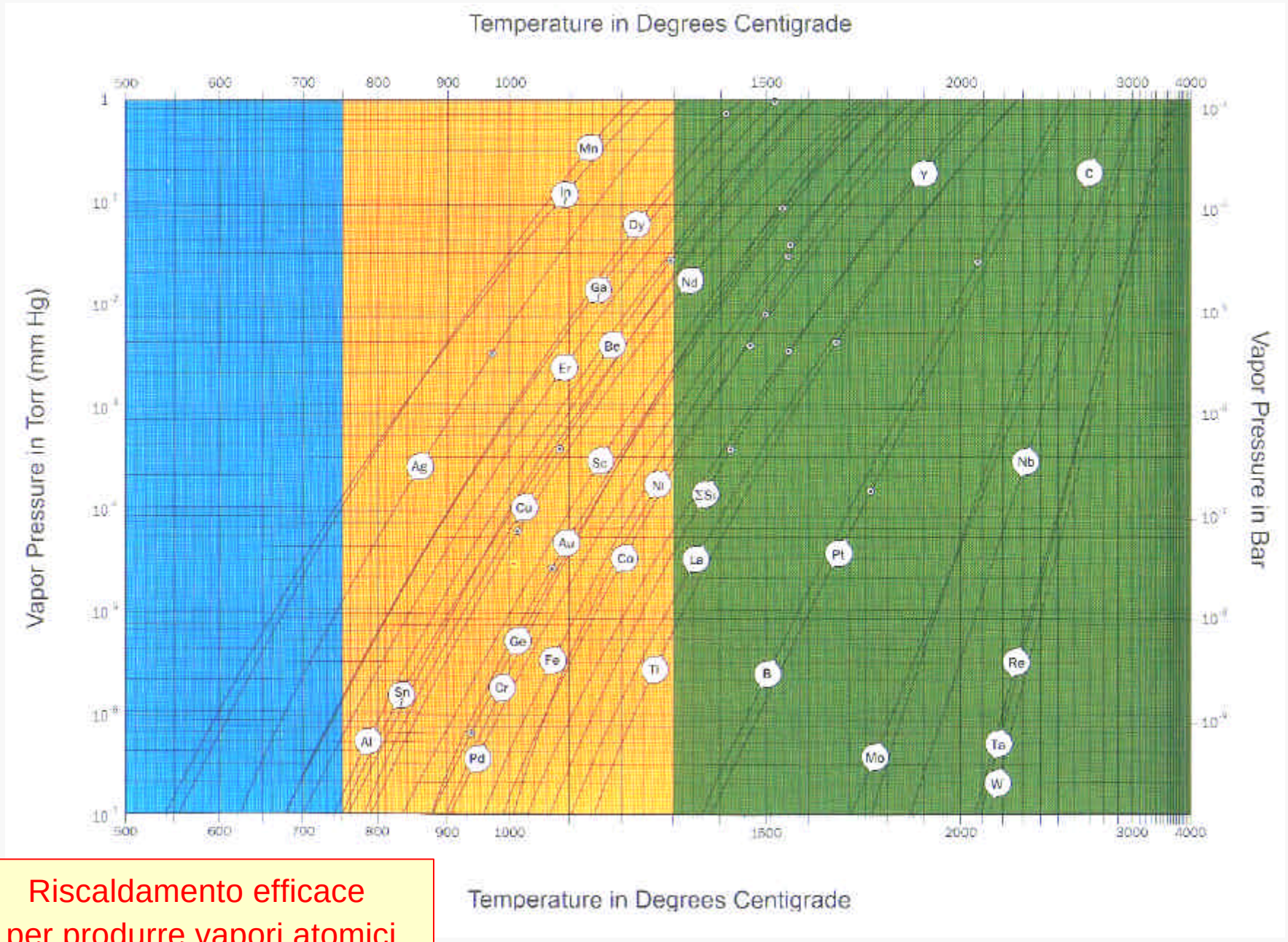

Riscaldamento efficace
per produrre vapori atomici
(es. vaporizzazione)

Molecular Beam Epitaxy: MBE, MOMBE

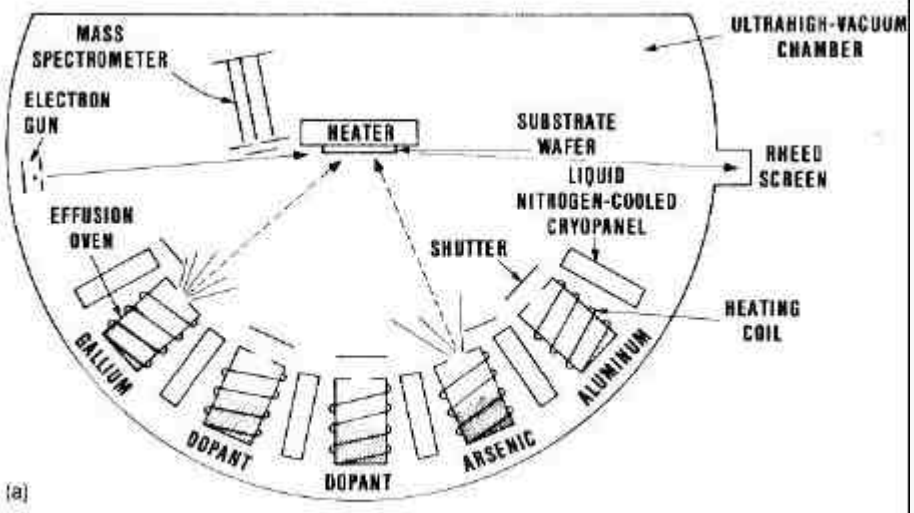

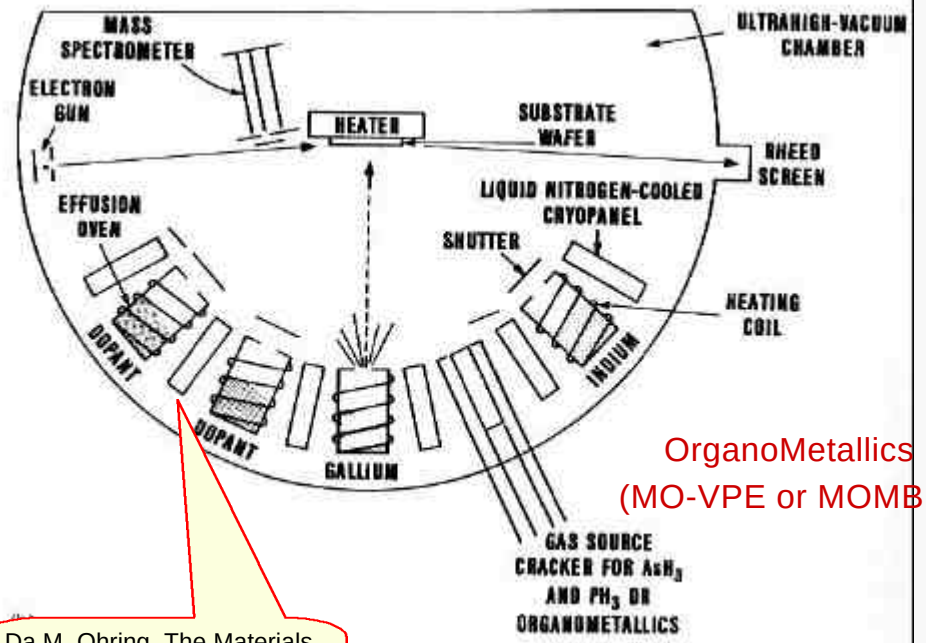

OrganoMetallics
(MO-VPE or MOMBE)

Da M. Ohring, The Materials Science of Thin Films, Academic (1992)

Elementi chiave MBE:

- alta pulizia (UHV, p = 10^{-10}mbar)
- basso growth rate in continua (~ 1 µm/h)
- operazione con *tutti* i semiconduttori

⇩

elevato controllo spessori a livello atomico
alta purezza
fabbricazione eterostrutture

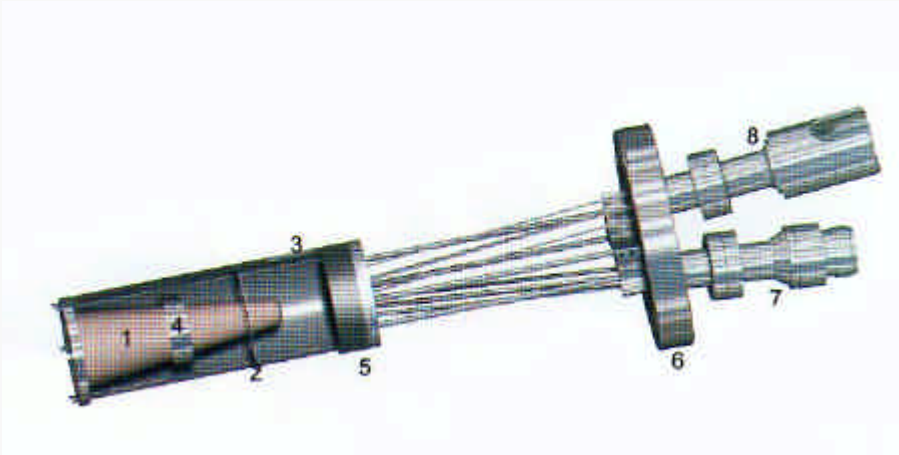

Forno effusivo (EPI):
alte temperature
--> reattività materiali?
--> pulizia?

Crescita di monostrati via MBE

Consider now a substrate positioned a distance l from a source aperture of area A, with $\phi = 0$. An expression for the number of evaporant species striking the substrate is

$$\dot{R} = \frac{3.51 \times 10^{22} PA}{\pi l^2 (MT)^{1/2}} \text{ molecules/cm}^2\text{-sec}. \qquad (7\text{-}13)$$

As an example, consider a Ga source in a system where $A = 5$ cm^2 and $l = 12$ cm. At $T = 900$ °C the vapor pressure $P_{Ga} \approx 1 \times 10^{-4}$ torr, and substituting $M_{Ga} = 70$, the arrival rate of Ga at the substrate is calculated to be 1.35×10^{14} atoms/cm^2-sec. The As arrival rate is usually much higher, and, therefore, film deposition is controlled by the Ga flux. An average monolayer of GaAs is 2.83 Å thick and contains $\sim 6.3 \times 10^{14}$ Ga atoms/cm^2. Hence, the growth rate is calculated to be $(1.35 \times 10^{14})/(6.3 \times 10^{14}) \times 2.83 \times 60 = 36$ Å/min, a rather low rate when compared with VPE.

Da M. Ohring, The Materials Science of Thin Films, Academic (1992)

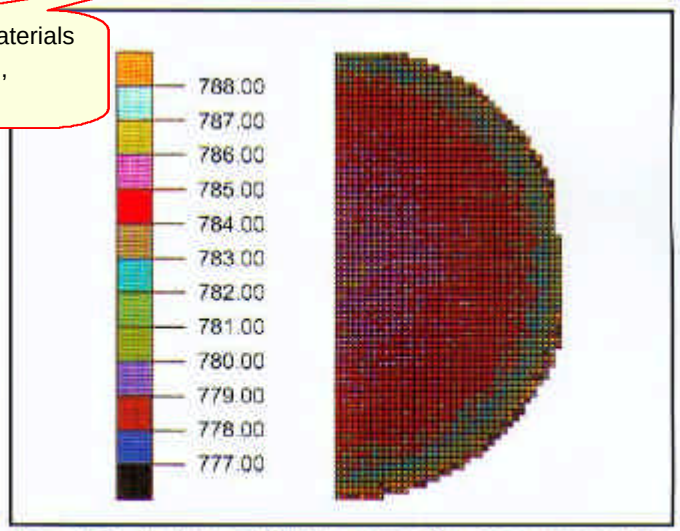

Figure 4-3 Thickness uniformity across a 3" wafer represented as a mapping of quantum well photoluminescence. The MQW structure was grown using a SUMO Ga cell in a MOD GEN II system. Uniformity better than ±1% was achieved. Data courtesy R. Sacks, Ohio State University and K. Stair, Northwestern University.

Crescita di monostrati
controllabile con diagnostiche in-situ
(es. RHEED)

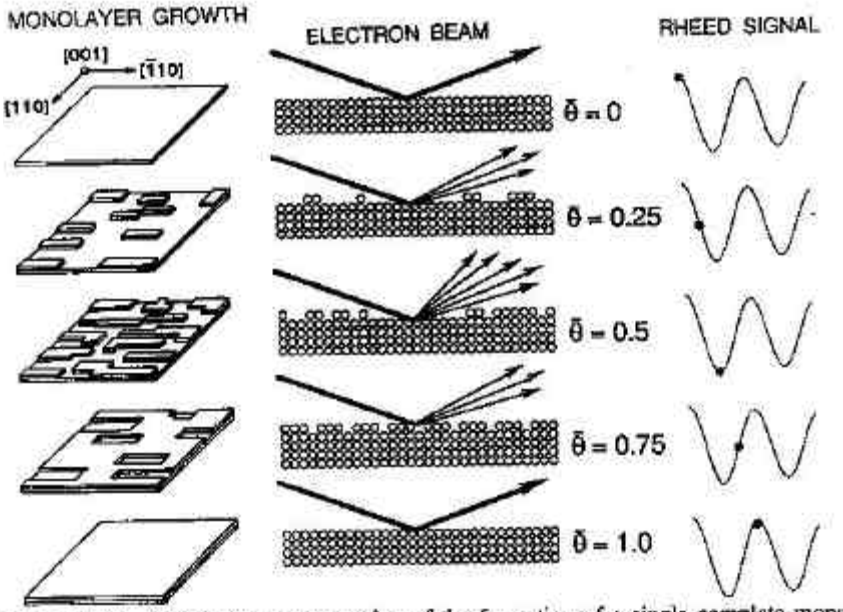

Figure 7-22. Real space representation of the formation of a single complete monolayer; θ is the fractional layer coverage; corresponding RHEED oscillation signal is shown.

Omogeneità su larga scala
(ind. wafer da 8", o più!!)

Sputtering (e bombardamento di cariche)

Particelle cariche (ioni od elettroni) accelerati verso la superficie di un target solido --> desorbimento (via numerosi processi) --> vaporizzazione (*non solo elementare*)

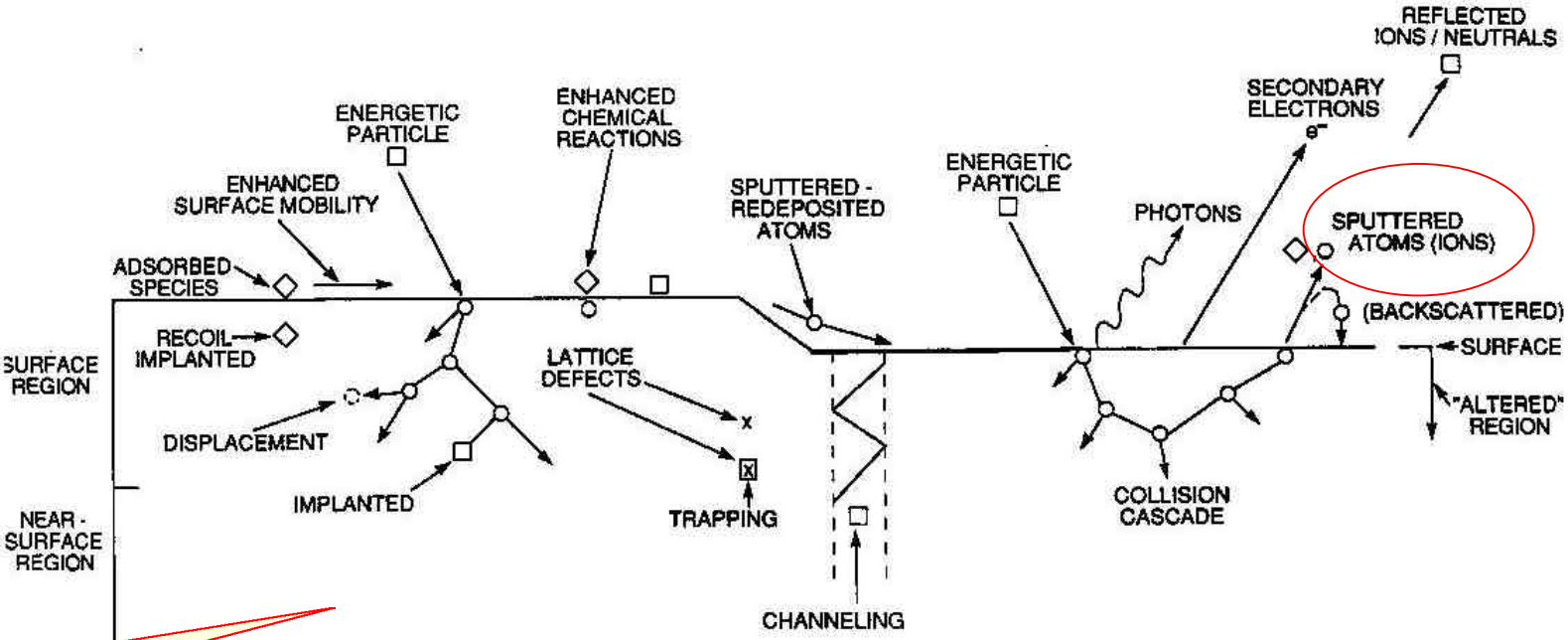

Da M. Ohring, The Materials Science of Thin Films, Academic (1992)

-16. Depiction of energetic particle bombardment effects on surfaces and growing films. (From Ref. 18).

Punti di forza principali:

- efficienza anche con materiali “refrattari”, es. ceramiche ed alcuni metalli con alta T_{vap}
- alti growth rate (fino a diversi µm/h)

DC, RF, Magnetron sputtering

Sputtering: cariche (accelerate) prodotte da plasma, tipicamente di gas inerte, prodotto in *continua* (DC) o con *radiofrequenza* (RF)

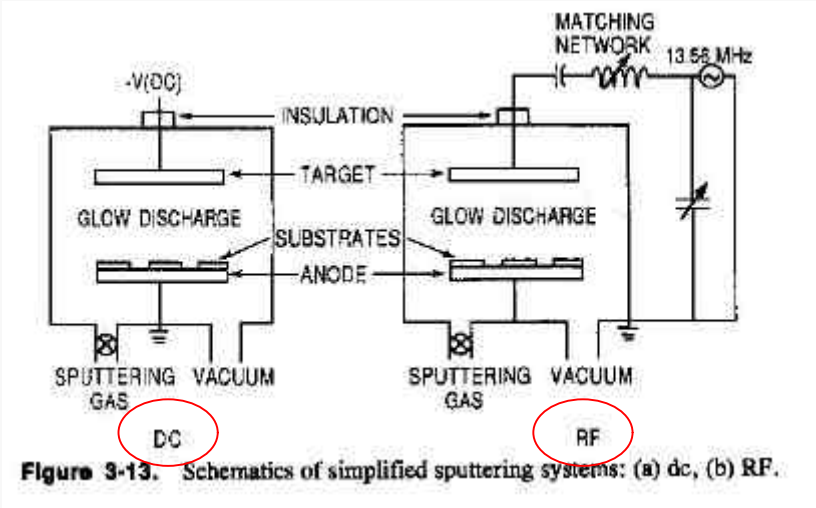

Figure 3-13. Schematics of simplified sputtering systems: (a) dc, (b) RF.

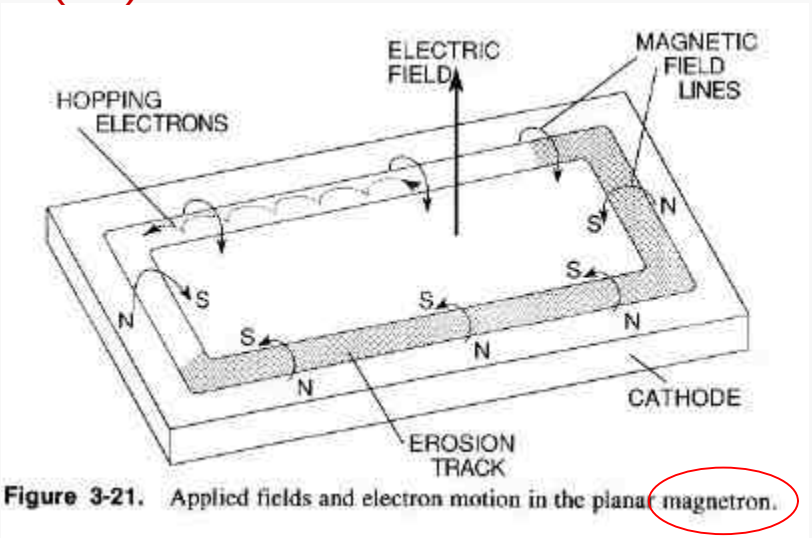

Figure 3-21. Applied fields and electron motion in the planar magnetron.

Campi magnetici aumentano ionizz. collisionale

Table 3-4. Sputtering Yield Data for Metals (atoms/ion)

Sputtering Gas Energy (keV)	He 0.5	Ne 0.5	Ar 0.5	Kr 0.5	Xe 0.5	Ar 1.0	Ar Threshold Voltage (eV)
Ag	0.20	1.77	3.12	3.27	3.32	3.8	15
Al	0.16	0.73	1.05	0.96	0.82	1.0	13
Au	0.07	1.08	2.40	3.06	3.01	3.6	20
Be	0.24	0.42	0.51	0.48	0.35		15
C	0.07	—	0.12	0.13	0.17		
Co	0.13	0.90	1.22	1.08	1.08		25
Cu	0.24	1.80	2.35	2.35	2.05	2.85	17
Fe	0.15	0.88	1.10	1.07	1.00	1.3	20
Ge	0.08	0.68	1.1	1.12	1.04		25
Mo	0.03	0.48	0.80	0.87	0.87	1.13	24
Ni	0.16	1.10	1.45	1.30	1.22	2.2	21
Pt	0.03	0.63	1.40	1.82	1.93		25
Si	0.13	0.48	0.50	0.50	0.42	0.6	
Ta	0.01	0.28	0.57	0.87	0.88		26
Ti	0.07	0.43	0.51	0.48	0.43		20
W	0.01	0.28	0.57	0.91	1.01		33

Principali svantaggi sputtering:

- presenza di gas ambiente (per il plasma)
  --> scarsa purezza
- possibilità backscattering
  --> danneggiamento film
- scarsa efficacia atomizzazione
  --> scarso controllo crescita

Confronto vaporizzazione/sputtering

Da M. Ohring, The Materials Science of Thin Films, Academic (1992)

Evaporation	Sputtering
A. Production of Vapor Species	
1. Thermal evaporation mechanism	1. Ion bombardment and collisional momentum transfer
2. Low kinetic energy of evaporant atoms (at 1200 K, $E = 0.1$ eV)	2. High kinetic energy of sputtered atoms ($E = 2$–30 eV)
3. Evaporation rate (Eq. 3-2) (for $M = 50$, $T = 1500$ K, and $P_e = 10^{-3}$) $\approx 1.3 \times 10^{17}$ atoms/cm^2-sec.	3. Sputter rate (at 1 mA/cm^2 and $S = 2$) $\approx 3 \times 10^{16}$ atoms/cm^2-sec
4. Directional evaporation according to cosine law	4. Directional sputtering according to cosine law at high sputter rates
5. Fractionation of multicomponent alloys, decomposition, and dissociation of compounds	5. Generally good maintenance of target stoichiometry, but some dissociation of compounds.
6. Availability of high evaporation source purities	6. Sputter targets of all materials are available; purity varies with material
B. The Gas Phase	
1. Evaporant atoms travel in high or ultrahigh vacuum ($\sim 10^{-6}$–10^{-10} torr) ambient	1. Sputtered atoms encounter high-pressure discharge region ($\sim$ 100 mtorr)
2. Thermal velocity of evaporant 10^5 cm/sec	2. Neutral atom velocity $\sim 5 \times 10^4$ cm/sec
3. Mean-free path is larger than evaporant–substrate spacing. Evaporant atoms undergo no collisions in vacuum	3. Mean-free path is less than target–substrate spacing. Sputtered atoms undergo many collisions in the discharge
C. The Condensed Film	
1. Condensing atoms have relatively low energy	1. Condensing atoms have high energy
2. Low gas incorporation	2. Some gas incorporation
3. Grain size generally larger than for sputtered film	3. Good adhesion to substrate
4. Few grain orientations (textured films)	4. Many grain orientations

Ablazione e deposizione laser impulsata (PLAD)

Interazione fascio laser impulsato/bulk solido
--> *ablazione* (vaporizzazione) localizzata materiale

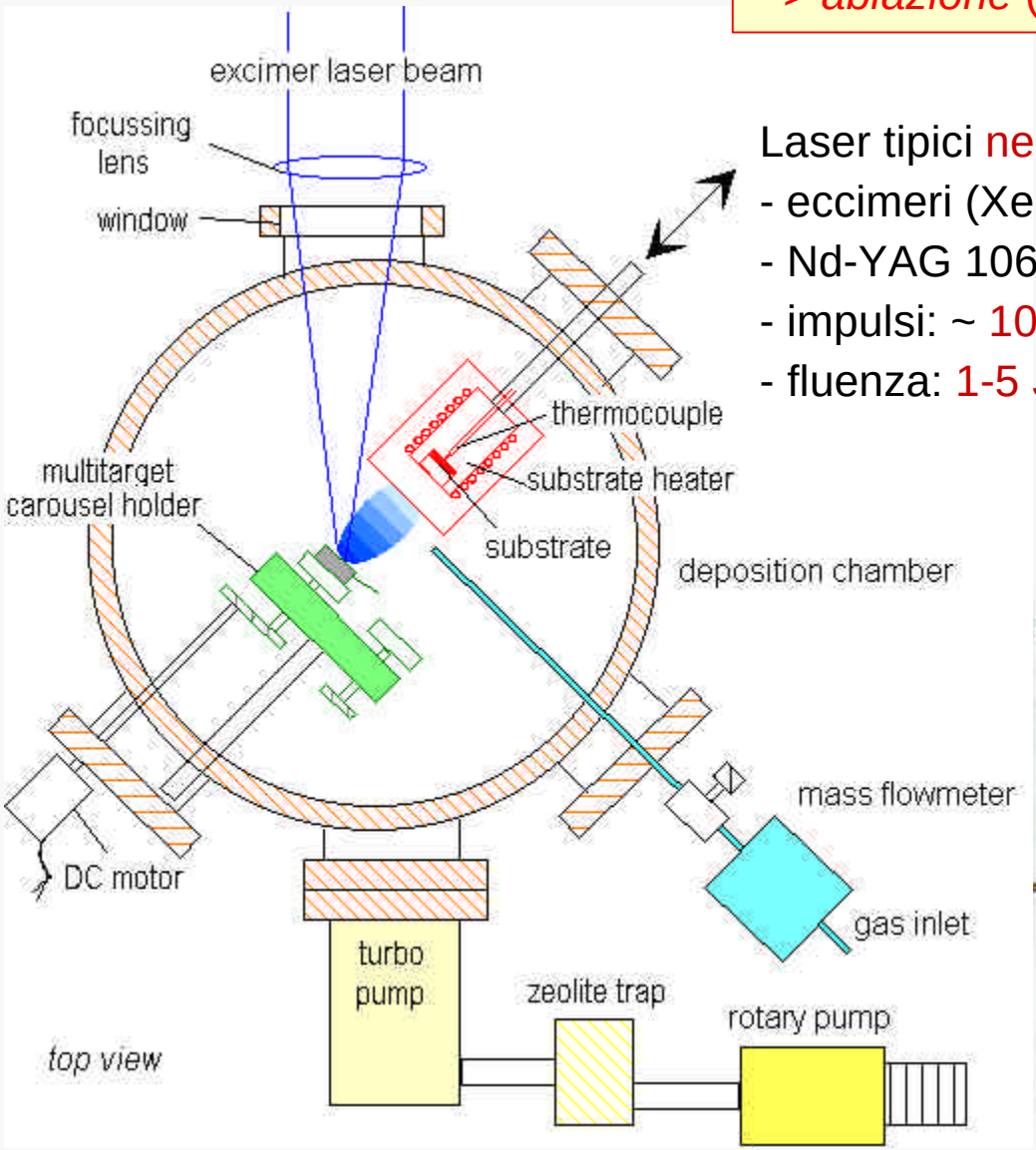

Laser tipici nell'UV:
- eccimeri (XeCl 308nm, KrF 248nm, ArF 193nm,…)
- Nd-YAG 1064 nm (III o IV armonica nell'UV)
- impulsi: ~ 10 ns (ma anche sub-ns)
- fluenza: 1-5 J/cm^2 (cioè centinaia di MW/cm^2)

Processo impulsato e tempi caratt.

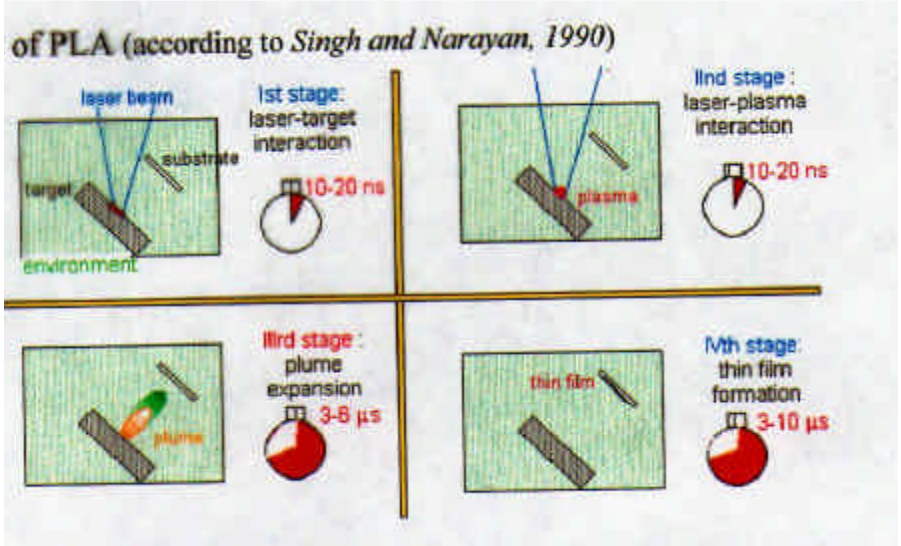

Accoppiamento laser UV/target

Processi di assorbimento di origine elettronica (anche con rottura di legami)

--> ablazione fredda

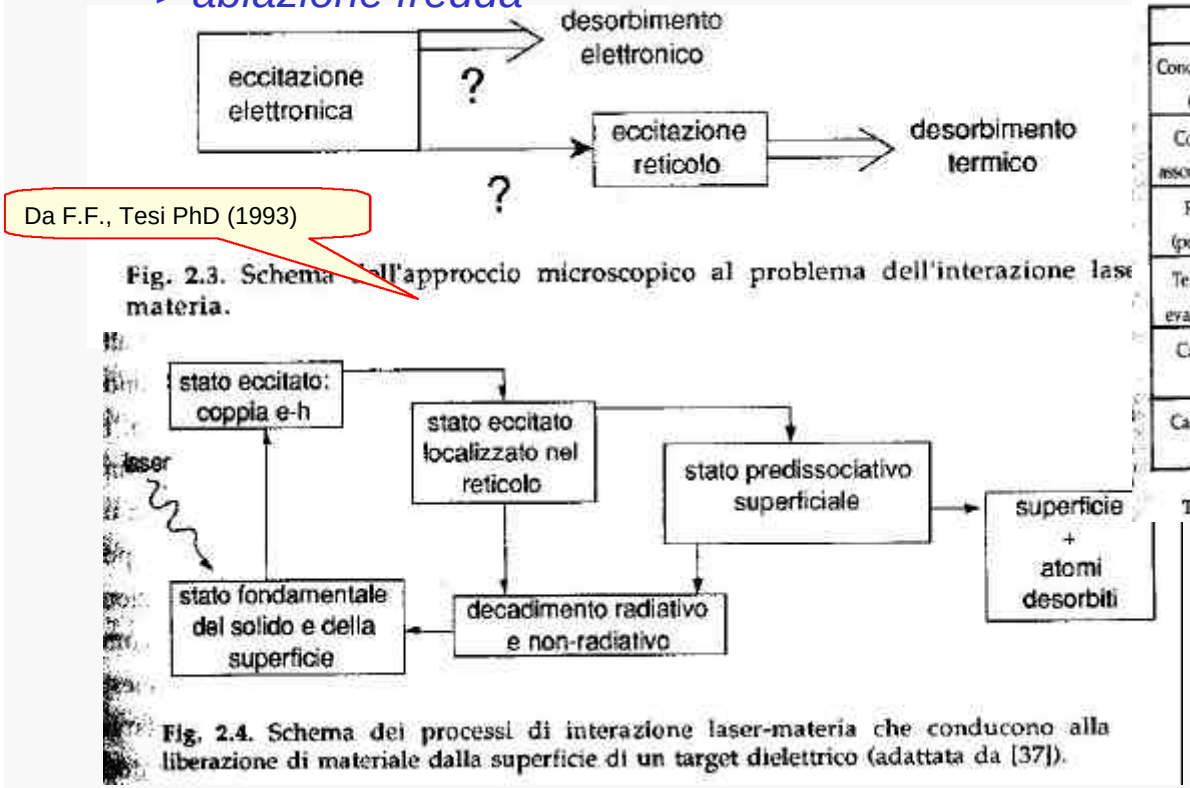

Da F.F., Tesi PhD (1993)

Fig. 2.3. Schema dell'approccio microscopico al problema dell'interazione lase materia.

Fig. 2.4. Schema dei processi di interazione laser-materia che conducono alla liberazione di materiale dalla superficie di un target dielettrico (adattata da [37]).

Materiale	YBCO	Si	Ni
Conduttività termica ($W\,cm^{-1}\,K^{-1}$)	0.025	$1600xT^{-1.23}$, T<1370 K 0.2, T>1370 K	$11xT^{-0.4}$, T<630 K $0.08xT^{0.3}$, 630<T<1726 K
Coefficiente di assorbimento (cm^{-1})	$1.75x10^5$	$>1.5x10^6$	$1.0x10^6$
Riflettività (per λ_L=308 nm)	0.11	0.59 0.73 (fase liquida)	0.40 0.70 (fase liquida)
Temperatura di evaporazione (K)	1900	3400	3187
Calore latente (J/cm^3)	14940	4206	2660
Calore specifico ($J/cm^3\,K$)	2.46	$2xT^{-3.68}$	$0.72xT^{0.3}$, T<630 K $0.5xT^{0.3}$, T>630 K

Tab. 2.1. Valori dei parametri termofisici ed ottici per diversi materiali (da [52, 53]).

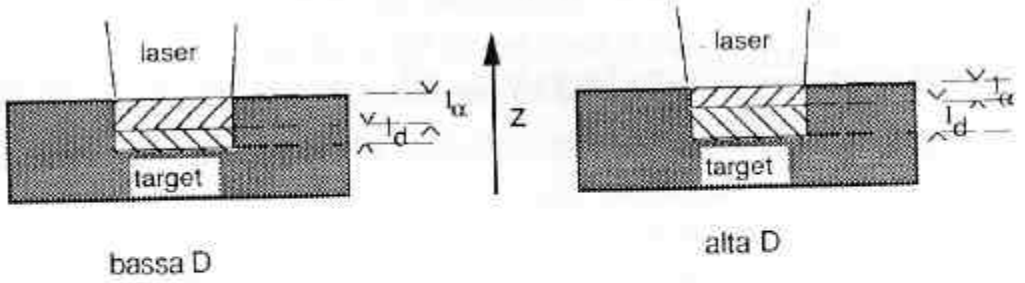

Fig. 2.7. Range di assorbimento di radiazione l_α e di diffusione del calore l_d in materiali con bassa ed alta diffusività termica D (a sinistra e destra nella figura, rispettivamente); indicato è anche l'asse z considerato nel testo.

Alcuni vantaggi della PLAD:
- grande efficacia con ogni mat.
- riscaldamento *molto* localizzato

Peculiarità PLAD

2.3.2 Stima semiempirica della profondità di ablazione.

Una stima della profondità di ablazione può essere data in modo semiempirico considerando il bilancio tra l'energia assorbita dal target e quella necessaria a produrne la vaporizzazione. Tenendo conto delle perdite per irraggiamento e conduzione (E_{cond}) e delle perdite dovute all'assorbimento da parte del plasma che si forma sopra la superficie (E_{pl}), secondo i processi che saranno discussi nei prossimi paragrafi, l'equazione di bilancio si scrive [29]:

$$(1 - R)\left(I_L - \frac{E_{cond} + E_{pl}}{S}\right) = \Delta z\,(\rho\, C_p\, \Delta T + L) \qquad (2.7)$$

con:

R : riflettività del target;
Δz : spessore di materiale ablato;
ΔT : aumento di temperatura che conduce all'ablazione;
S : superficie irraggiata dal laser
L : calore latente di vaporizzazione.

L'approssimazione semiempirica consiste nell'introdurre la densità d'energia di soglia dell'ablazione I_{Lthr} ponendola pari alle perdite di energia per unità di superficie, ottenendo:

$$\Delta z = (1 - R)\frac{I_L - I_{Lthr}}{\rho\, C_p\, \Delta T + L} \qquad (2.8)$$

Lo spessore di materiale ablato per $I_L = 2.0$ J/cm² ottenuto dalla (2.8) utilizzando i parametri riportati in **Tab. 2.1** per l'YBCO e ponendo $I_{L,thr} = 0.3$ J/cm² (misurato nel corso dei nostri esperimenti) è $\Delta z \approx 700$ Å, simile a quello da me determinato dalla misura della quantità di materiale ablata per l'YBCO [14] corrispondente alla rimozione di ≈ 0.5 μg di materiale per colpo laser.

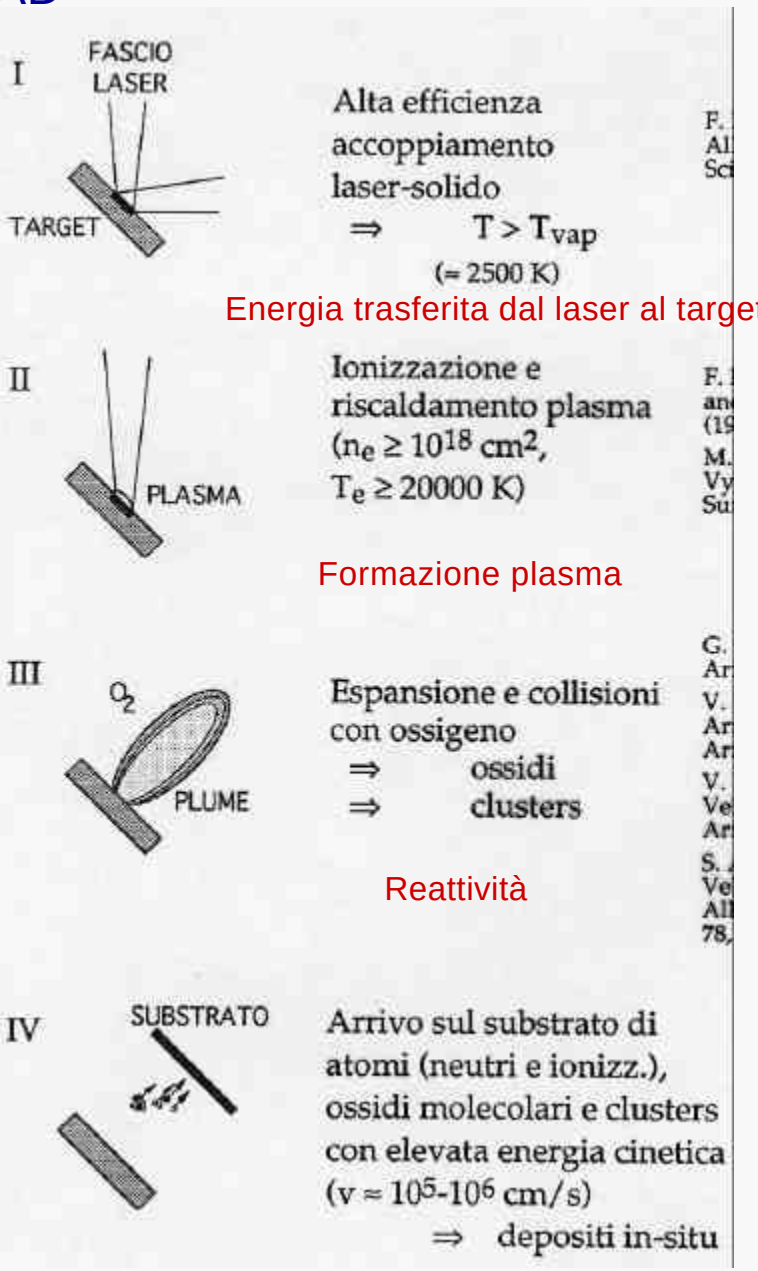

Ulteriori vantaggi PLAD:

- elevato tasso di ablazione per laser shot
- elevata energia cinetica particelle ablate
- elevata direzionalità
- possibilità reazioni collisionali (gas ambiente)

Limiti PLAD

PLAD diffusa in ambito di laboratorio per film di materiali “difficili” (es. ceramiche supercoduttrici, ferroelettriche, ferromagnetiche, ossidi,...)
Può essere usata anche per formare nanoparticelle (CNT, Si-nanocrystals,…)

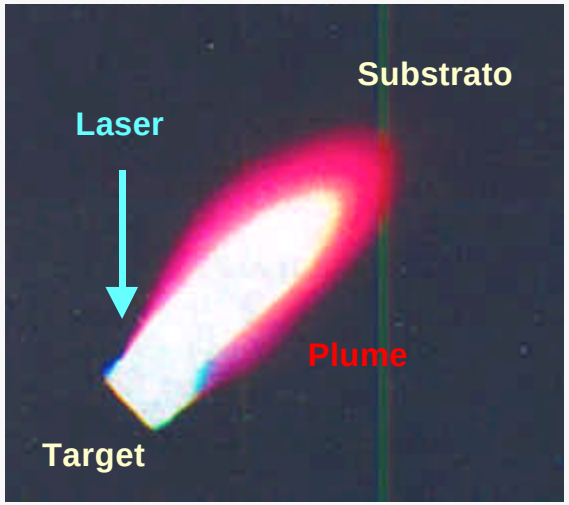

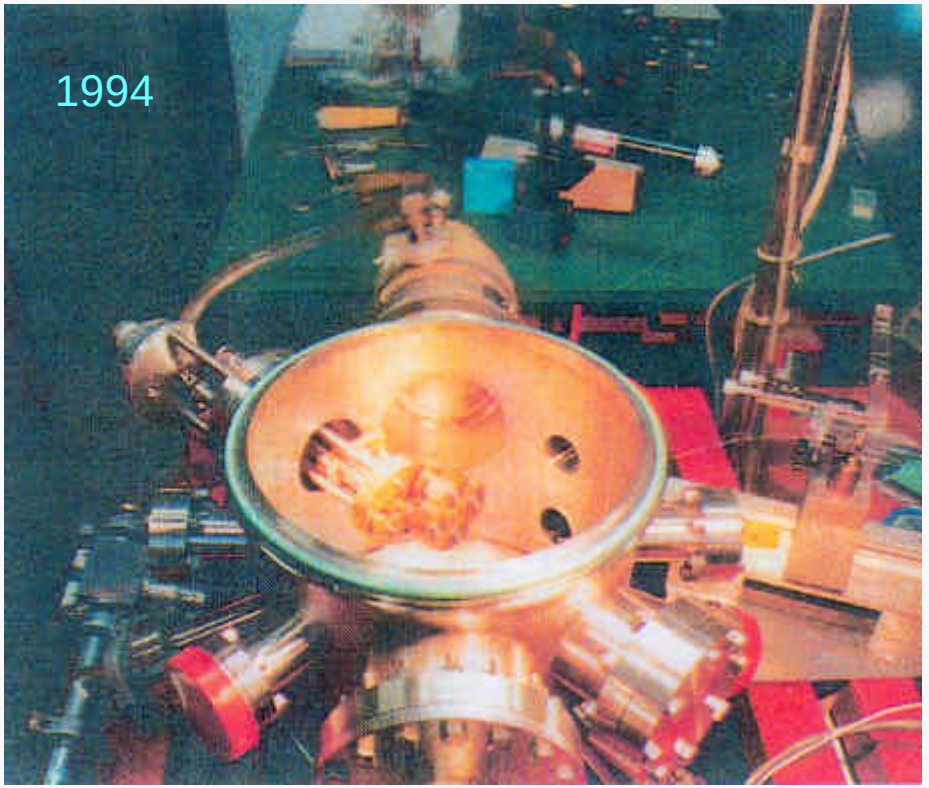

Alcuni svantaggi PLAD:
- copertura piccole superfici (~ cm^2)
- scarsa omogeneità superficiale e formazione *droplets*
- difficile diffusione industriale (laser)
- scarsa resa complessiva

Tecniche chimiche: Chemical Vapor Deposition (CVD)

Da M. Ohring, The Materials Science of Thin Films, Academic (1992)

Reazioni in fase di vapore a partire da *precursori* di varia natura (solida, gassosa, liquida) usate per produrre i componenti elementari del film

Alcune reazioni per metalli e semiconduttori:

4.2.1. Pyrolysis

Pyrolysis involves the thermal decomposition of such gaseous species as hydrides, carbonyls, and organometallic compounds on hot substrates. Commercially important examples include the high-temperature pyrolysis of silane to produce polycrystalline or amorphous silicon films, and the low-temperature decomposition of nickel carbonyl to deposit nickel films.

$$SiH_{4(g)} \rightarrow Si_{(s)} + 2H_{2(g)} \quad (650\ ^\circ C), \quad \text{Si} \quad (4\text{-}1)$$

$$Ni(CO)_{4(g)} \rightarrow Ni_{(s)} + 4CO_{(g)} \quad (180\ ^\circ C), \quad \text{Ni} \quad (4\text{-}2)$$

Interestingly, the latter reaction is the basis of the Mond process, which has been employed for over a century in the metallurgical refining of Ni.

4.2.2. Reduction

These reactions commonly employ hydrogen gas as the reducing agent to effect the reduction of such gaseous species as halides, carbonyl halides, oxyhalides, or other oxygen-containing compounds. An important example is the reduction of $SiCl_4$ on single-crystal Si wafers to produce epitaxial Si films according to the reaction

$$SiCl_{4(g)} + 2H_{2(g)} \rightarrow Si_{(s)} + 4HCl_{(g)} \quad (1200\ ^\circ C). \quad \text{Si} \quad (4\text{-}3)$$

Refractory metal films such as W and Mo have been deposited by reducing the corresponding hexafluorides, e.g.,

$$WF_{6(g)} + 3H_{2(g)} \rightarrow W_{(s)} + 6HF_{(g)} \quad (300\ ^\circ C). \quad \text{W} \quad (4\text{-}4)$$

$$MoF_{6(g)} + 3H_{2(g)} \rightarrow Mo_{(s)} + 6HF_{(g)} \quad (300\ ^\circ C). \quad \text{Mo} \quad (4\text{-}5)$$

Tungsten films deposited at low temperatures have been actively investigated as a potential replacement for aluminum contacts and interconnections in integrated circuits. Interestingly, WF_6 gas reacts directly with exposed silicon surfaces, depositing thin W films while releasing the volatile SiF_4 by-product. In this way silicon contact holes can be selectively filled with tungsten while leaving neighboring insulator surfaces uncoated.

4.2.3. Oxidation

Two examples of important oxidation reactions are

$$SiH_{4(g)} + O_{2(g)} \rightarrow SiO_{2(s)} + 2H_{2(g)} \quad (450\ ^\circ C), \quad SiO_2 \quad (4\text{-}6)$$

$$4PH_{3(g)} + 5O_{2(g)} \rightarrow 2P_2O_{5(s)} + 6H_{2(g)} \quad (450\ ^\circ C). \quad (4\text{-}7)$$

The deposition of SiO_2 by Eq. 4-6 is often carried out at a stage in the processing of integrated circuits where higher substrate temperatures cannot be tolerated. Frequently, about 7% phosphorous is simultaneously incorporated in the SiO_2 film by the reaction of Eq. 4-7 in order to produce a glass film that flows readily to produce a planar insulating surface, i.e., "planarization."

In another process of technological significance, SiO_2 is also produced by the oxidation reaction

$$SiCl_{4(g)} + 2H_{2(g)} + O_{2(g)} \rightarrow SiO_{2(s)} + 4HCl_{(g)} \quad (1500\ ^\circ C). \quad (4\text{-}8) \quad SiO_2$$

The eventual application here is the production of optical fiber for communications purposes. Rather than a thin film, the SiO_2 forms a cotton-candy-like deposit consisting of soot particles less than 1000 Å in size. These are then consolidated by elevated temperature sintering to produce a fully dense silica rod for subsequent drawing into fiber. Whether silica film deposition or soot formation occurs is governed by process variables favorable to heterogeneous or homogeneous nucleation, respectively. Homogeneous soot formation is essentially the result of a high $SiCl_4$ concentration in the gas phase.

4.2.4. Compound Formation

A variety of carbide, nitride, boride, etc., films and coatings can be readily produced by CVD techniques. What is required is that the compound elements exist in a volatile form and be sufficiently reactive in the gas phase. Examples of commercially important reactions include

$$SiCl_{4(g)} + CH_{4(g)} \rightarrow SiC_{(s)} + 4HCl_{(g)} \quad (1400\ ^\circ C), \quad (4\text{-}9) \quad \text{SiC}$$

$$TiCl_{4(g)} + CH_{4(g)} \rightarrow TiC_{(s)} + 4HCl_{(g)} \quad (1000\ ^\circ C), \quad (4\text{-}10)$$

$$BF_{3(g)} + NH_{3(g)} \rightarrow BN_{(s)} + 3HF_{(g)} \quad (1100\ ^\circ C) \quad (4\text{-}11) \quad \text{BN}$$

for the deposition of hard, wear-resistant surface coatings. Films and coatings of compounds can generally be produced through a variety of precursor gases and reactions. For example, in the much studied SiC system, layers were first

Esempi di reazioni per CVD

produced in 1909 through reaction of $SiCl_4 + C_6H_6$ (Ref. 8). Subsequent reactant combinations over the years have included $SiCl_4 + C_3H_8$, $SiBr_4 + C_2H_4$, $SiCl_4 + C_6H_{14}$, $SiHCl_3 + CCl_4$, and $SiCl_4 + C_6H_5CH_3$, to name a few, as well as volatile organic compounds containing both silicon and carbon in the same molecule (e.g., CH_3SiCl_3, CH_3SiH_3, $(CH_3)_2SiCl_2$, etc.). Although the deposit is nominally SiC in all cases, resultant properties generally differ because of structural, compositional, and processing differences.

Impermeable insulating and passivating films of Si_3N_4 that are used in integrated circuits can be deposited at 750 °C by the reaction

$$3SiCl_2H_{2(g)} + 4NH_{3(g)} \rightarrow Si_3N_{4(s)} + 6H_{2(g)} + 6HCl_{(g)}. \quad (4\text{-}12)$$

Si_3N_4

The necessity to deposit silicon nitride films at lower temperatures has led to alternative processing involving the use of plasmas. Films can be deposited below 300 °C with SiH_4 and NH_3 reactants, but considerable amounts of hydrogen are incorporated into the deposits.

4.2.5. Disproportionation

Disproportionation reactions are possible when a nonvolatile metal can form volatile compounds having different degrees of stability, depending on the temperature. This manifests itself in compounds, typically halides, where the metal exists in two valence states (e.g., GeI_4 and GeI_2) such that the lower-valent state is more stable at higher temperatures. As a result, the metal can be transported into the vapor phase by reacting it with its volatile, higher-valent halide to produce the more stable lower-valent halide. The latter disproportionates at lower temperatures to produce a deposit of metal while regenerating the higher-valent halide. This complex sequence can be simply described by the reversible reaction

$$2GeI_{2(g)} \underset{600\ °C}{\overset{300\ °C}{\rightleftharpoons}} Ge_{(s)} + GeI_{4(g)} \quad (4\text{-}13)$$

and realized in systems where provision is made for mass transport between hot and cold ends. Elements that have lent themselves to this type of transport reaction include aluminum, boron, gallium, indium, silicon, titanium, zirconium, beryllium, and chromium. Single-crystal films of Si and Ge were grown by disproportionation reactions in the early days of CVD experimentation on semiconductors employing reactors such as that shown in Fig. 4-2. The enormous progress made in this area is revealed here.

4.2.6. Reversible Transfer

Chemical transfer or transport processes are characterized by a reversal in the reaction equilibrium at source and deposition regions maintained at different temperatures within a single reactor. An important example is the deposition of single-crystal (epitaxial) GaAs films by the chloride process according to the reaction

$$As_{4(g)} + As_{2(g)} + 6GaCl_{(g)} + 3H_{2(g)} \underset{850\ °C}{\overset{750\ °C}{\rightleftharpoons}} 6GaAs_{(s)} + 6HCl_{(g)}. \quad (4\text{-}14)$$

Here $AsCl_3$ gas from a bubbler transports Ga toward the substrates in the form of GaCl vapor. Subsequent reaction with As_4 causes deposition of GaAs.

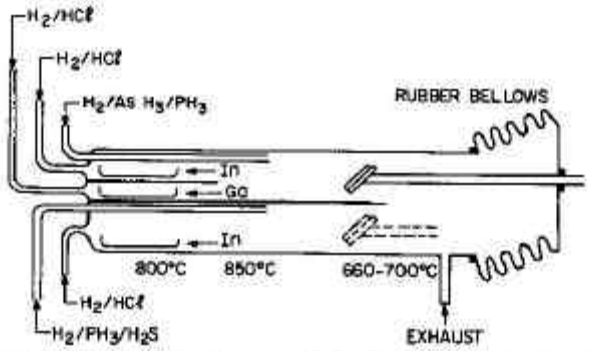

Figure 4-3. Schematic of atmospheric CVD reactor used to grow GaAs and other compound semiconductor films by the hydride process. (Reprinted with permission from Ref. 10).

Alternatively, in the hydride process, As is introduced in the form of AsH_3 (arsine), and HCl serves to transport Ga. Both processes essentially involve the same gas-phase reactions and are carried out in similar reactors, shown schematically in Fig. 4-3. What is significant is that single-crystal, *binary* (primarily GaAs and InP but also GaP and InAs) as well as *ternary* (e.g., (Ga, In)As and Ga(As, P)) compound films have been grown by these vapor phase epitaxy (VPE) processes. Similarly, in addition to binary and ternary semiconductor films, *quaternary* epitaxial films containing controlled amounts of Ga, In, As, and P have been deposited by the hydride VPE process. Combinations of gas mixtures and more complex reactors are required in this case to achieve the desired stoichiometries. The resulting films are the object of intense current research and development activity in a variety of optoelectronic devices (e.g., lasers and detectors). For quaternary alloy deposition by the hydride process, single-crystal InP substrates are employed. Gas-phase source reactions include

$$2AsH_3 \rightleftarrows As_2 + 3H_2, \quad \text{As}$$
$$2PH_3 \rightleftarrows P_2 + 3H_2, \quad \text{P}$$
$$2HCl + 2In \rightleftarrows 2InCl + H_2,$$
$$2HCl + 2Ga \rightleftarrows 2GaCl + H_2. \quad (4\text{-}15)$$

Deposition reactions at substrates include

$$2GaCl + As_2 + H_2 \rightleftarrows 2GaAs + 2HCl, \quad \text{GaAs}$$
$$2GaCl + P_2 + H_2 \rightleftarrows 2GaP + 2HCl, \quad \text{GaP}$$
$$2InCl + P_2 + H_2 \rightleftarrows 2InP + 2HCl, \quad \text{InP}$$
$$2InCl + As_2 + H_2 \rightleftarrows 2InAs + 2HCl. \quad \text{InAs} \quad (4\text{-}16)$$

GaAs

Da M. Ohring, The Materials Science of Thin Films, Academic (1992)

Anche Plasma-Enhanced CVD!! (vedi fabbricazione nanotubi)

Liquid Phase Epitaxy (LPE) e Sol-Gel

LPE: deposizione da soluzione sopra-satura

techniques. LPE involves the precipitation of a crystalline film from a supersaturated melt onto the parent substrate, which serves as both the template for epitaxy and the physical support for the heterostructure. The process can be understood by referring to the GaAs binary-phase diagram on p. 31. Consider a Ga-rich melt containing 10 at% As. When heated above 950°C, all of the As dissolves. If the melt is cooled below the liquidus temperature into the two-phase field, it becomes supersaturated with respect to As. Only a melt of lower than the original As content can now be in equilibrium with GaAs. The excess As is, therefore, rejected from solution in the form of GaAs that grows epitaxially on a suitably placed substrate. Many readers will appreciate that the

Da M. Ohring, The Materials Science of Thin Films, Academic (1992)

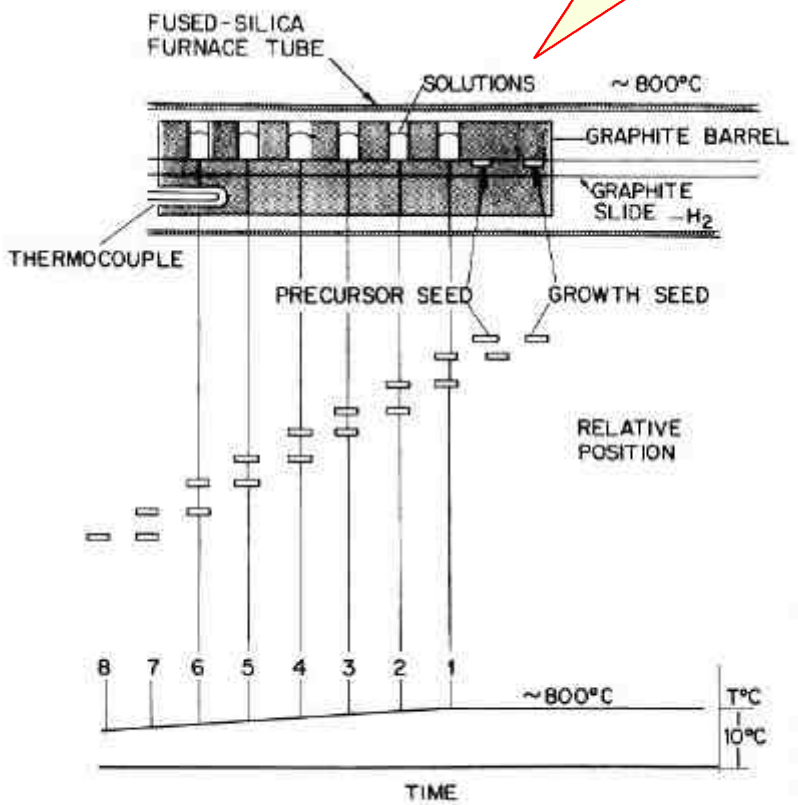

Figure 7-17. Schematic of LPE reactor. (Courtesy of M. B. Panish, AT&T Bell Laboratories.)

Sol-Gel: deposizione da precursori sciolti in solventi gelificanti (adatta anche per ceramiche)

Alcuni vantaggi dei metodi chimici:
- economia
- scalabilità
- resa

Principali svantaggi dei metodi chimici:
- scarso controllo di omogeneità chimica, srutturale e morfologica
- applicabilità limitata ad alcune classi di materiali
- necessità di vari passaggi intermedi e scarsa integrabilità